Journal of New Materials for Electrochemical Systems 8, 305-315 (2005)

The Effect of High Positive Potentials on the Different Charge Transport and Charge Transfer Parameters of Poly(O-Amnophenol) Modified Electrodes. A Study Using Cyclic Voltammetry, Steady-State Rotating Disc Electrode Voltammetry and AC Impedance Measurements

R. Tucceri

Instituto de Investigaciones Fisicoquímicas Teóricas y Aplicadas (INIFTA)
Facultad de Ciencias Exactas, Universidad Nacional de La Plata,
Sucursal 4, Casilla de Correo 16, (1900)- La Plata, Argentina.
Mailing Adress: R.I. Tucceri, Instituto de Investigaciones Fisicoquímicas Teóricas y Aplicadas (INIFTA), Sucursal 4, Casilla de Correo 16, (1900)- La Plata, Argentina.

(Received March 31, 2005 ; received in revised form January 06, 2006)

Abstract: *Cyclic Voltammetry was employed to prepare fresh poly(o-aminophenol) (POAP) films and also to degrade them quantitatively. Then, the different behaviour of freshly prepared and degraded POAP films was studied by Steady-State Rotating Disc Electrode Voltammetry and Electrochemical Impedance Spectroscopy, when a mediated redox reaction is taking place at the polymer-solution interface. With regard to the last technique, the resulting experimental impedance diagrams of these POAP films, contacting the p-benzoquinone/hydroquinone redox couple, were interpreted on the basis of the homogeneous impedance model described in M.A. Vorotyntsev, C. Deslouis, M.M. Musiani, B. Tribollet, K. Aoki, Electrochimica Acta, 44 (1999) 2105-2115. The different dependencies of the charge transfer and charge transport parameters on the degree of degradation of the polymer ($\theta_{Red,Max}$), were obtained. The different features of some of these dependencies (for instance, bulk electronic and ionic transport on $\theta_{Red,Max}$) were explained in terms of the different mechanisms of electron and proton transport in this polymer. Also, similar behaviours of the transversal charge transfer resistance at the metal-polymer interface $R_{m|f}$ (obtained by impedance spectroscopy) and the lateral resistance $\Delta R/R$ along the electrode (obtained by Surface Resistance measurements), as functions of $\theta_{Red,Max}$, were explained in terms of two different aspects of the electron motion at metal surfaces contacting a polymeric material. The results of this work allows one to demonstrate that after to subject POAP films to rough conditions, as in some of practical applications of POAP, ion and electron diffusion inside the film and rates of interfacial charge transfer processes, are strongly reduced. It should be expected that this deterioration process reduces drastically the efficiency of the material to act in practical applications.*

Key words : poly(o-aminophenol), mediation reaction, steady-state rotating disc electrode voltammetry, ac impedance measurements, charge transfer parameters, ion and electron diffusion.

INTRODUCTION

Oxidation of o-aminophenol on different electrode materials (gold, platinum, carbon, etc.) in aqueous acid medium was shown to form poly-o-aminophenol (POAP) [1-3]. This electroactive polymer has been characterised by using different electrochemical techniques [3-15]. The polymer exhibits its maximal electroactivity within the potential range -0.2 V < *E* < 0.5 V (*vs.* SCE) at pH values lower than 3 [8,10,12]. Recent spectroscopic results seem to indicate that phenoxazine units are produced during the oxidation/reduction of POAP [13]. Also, in a more recent paper [14] is demonstrated by using differ-

*To whom correspondence should be addressed: Fax: (54) (0221) 425-4642
E-Mail: rtucce@inifta.unlp.edu.ar

ent in situ techniques (FTIR spectroscopy, Probe Beam Deflection and UV-Vis and Raman signals) that the redox transition of POAP from its completely oxidised state to its completely reduced state occurs through two consecutive reactions, in which a charged intermediate species takes part. With regard to its practical applications, the material was used to study silver deposition [16] and also it was employed as both cation sensor [17,18] and biosensor [19-21]. Recently, the electrocatalytic oxidation of methanol at a glassy carbon electrode modified by a thin POAP film containing Pt, Pt-Ru and Pt-Sn microparticles [22] and the development of NO sensors based on hybrid film of POAP and Ni sulfonated phtalocyanine [23], were reported. In some of these practical applications, POAP is subjected to positive potentials exceeding the potential range corresponding to the maximal electroactivity (E > 0.5 V (*vs.* SCE)). In this connection, in previous works [24-26] it was demonstrated that when the positive potential limit is extended to values higher than 0.5 V (*vs.* SCE) an irreversible deterioration of POAP films occurs. Despite of these last works and considering the growing applications of POAP no much efforts have been made to study more deeply the POAP degradation, specially in relation to its effect in the interesting case where this polymer material contacts an electrolyte solution containing a redox substrate and a mediation reaction occurs at the polymer-electrolyte interface. The aim of this work was to apply the Electrochemical Impedance Spectroscopy (EIS) to analyse the effect of the gradual degradation of POAP on the different charge transport and charge transfer processes through a POAP film, from the metal to the solution, when a mediation reaction occurs at the polymer-electrolyte interface. Also, Cyclic Voltammetry (CV) and Rotating Disk Electrode Voltammetry (RDEV) were used to synthesize and characterize fresh and degraded POAP films. Experimental impedance diagrams were interpreted on the basis of an homogeneous impedance model, such as that developed by Vorotyntsev et al. [27] which describes the impedance behaviour of electroactive polymers in the presence of redox species able to be discharged at the polymer-solution interface. In this sense, this model described in [27] was employed within the potential range comprised between -0.2 V and 0.0 V, where the reduction of p-benzoquinone (redox active substrate) occurs through a rapid electron transfer mediation at the POAP-solution interface. Then, the different transport and transfer parameters of the polymer layer, extracted from the fitting of the experimental impedance diagrams, were represented as a function of the degree of polymer degradation. Some interfacial transport parameters obtained in the present work by employing the EIS technique were compared with those obtained by using Surface Resistance (SR) measurements in [25]. It is expected that the results of this work can help to exploit more successfully the restrictive stability conditions of POAP in its practical applications.

1. EXPERIMENTAL

1.1 The Gold Base Electrode

A conventional three electrodes cell was used for the experiments. A rotating disc gold electrode (RDGE) was used as base electrode. This RDGE consisted of a gold rod press-fitted with epoxy resin into a Teflon sleeve so as to leave a disc area 1 cm^2 exposed. The gold electrode was carefully polished with emery paper of decreasing grit size followed by alumina suspensions of size 1, 0.3 and 0.05 μm, respectively, until a mirror-like finish was obtained. Then, it was submitted to ultrasonic cleaning to remove residual abraded polishing material. In order to obtain a more specular gold surface, a gold film of about 100 nm of thickness was deposited by vacuum evaporation ($\sim 10^{-7}$ Torr) on the gold disc, following the procedure described in [28,29]. Then, POAP films were electrochemically deposited on the RDGE after deposition of the gold film, and this POAP modified electrode was employed as working electrode. A gold grid of large area was used as counter electrode. All the potentials reported in this work are referred to the SCE.

1.2 Synthesis of fresh and Degraded Poap films by Using CV

1.2.1 Freshly prepared POAP films

POAP films were grown on the above mentioned RDGE (after to deposit a 100 nm thick gold film) in the same way as described in [1,25,30]. These polymer films were obtained by immersing the RDGE in a 10^{-3} M orthoaminophenol + 0.4 M $NaClO_4$ + 0.1 M $HClO_4$ solution and cycling the potential between -0.25 and 0.8 V (*vs.* SCE) at a scan rate ν = 0.05 V s^{-1}. In order to obtain a measure of the polymer thickness, these POAP coated rotating disc gold electrodes were then rinsed and transferred to the supporting electrolyte solution (0.4 M $NaClO_4$ + 0.1 M $HClO_4$) free of monomer. Then, the voltammetric reduction charge $Q_{T,Red}$ in this last solution was determined by integration the cathodic current of the voltammetric response between -0.25 V and 0.5 V (*vs.* SCE) (ν = 0.01 V s^{-1}) [1]. After this, $Q_{T,Red}$ was considered as representative of the POAP thickness. In these experiments only thick POAP films were used to cover the gold surface ($Q_{T,Red}$ = 2.8 mC cm^{-2}). A comparison between the redox charge $Q_{T,Red}$ measured by CV and the thickness ϕ_p determined by ellipsometry was previously reported for POAP films [1]. The $Q_{T,Red}$ value given above corresponds to the value $\phi_p \sim$ 60 nm. Eleven POAP coated rotating disc gold electrodes, all of the same polymer thickness, were consecutively manufactured to perform the present experiments. Each one of the 11 POAP coated RDGEs was successively used as the working electrode in an individual experiment. The voltammetric response *j-E* of each of the POAP coated RDGE (immediately after growing the polymer film on the gold surface, that is, freshly prepared) was recorded. These records were performed

within the potential region of maximal electroactivity of POAP (-0.2 V < *E* < 0.5 V).

1.2.2 Degraded POAP films and their degree of degradation ($\theta_{Red,Max}$)

Degradation of POAP films was quantitatively controlled using CV. Each one of the POAP coated gold electrodes, after to be equilibrated within the potential region -0.2 < *E* < 0.5 V, was subjected to a potential cycling between the limits -0.2 V < *E* < E_{upl} with E_{upl} > 0.5 V, during different time periods [25]. This yields a gradual attenuation of the initial *j-E* response of the polymer. More precisely, the 11 POAP coated gold electrodes were split into three different groups. While the first group, including three samples, was subjected to potential cycles where E_{upl} = 1.0 V, the second and third ones, each involving four samples, were subjected to potential cycles where E_{upl} values of 0.8 V and 0.65 V, respectively. The first column of Table 1, indicates the three different groups. In the second one the E_{upl} value used for each group is indicated. The third column indicates the different cycling times at the corresponding E_{upl} value at which each sample of each group was subjected. Then, after these treatments, the positive potential limit was again restricted to the value *E* = 0.5 V and *j-E* responses, for each sample of the different groups, were again recorded within the potential window of maximal electroactivity of POAP. $Q_{T,Red}$, values corresponding to the completely reduced POAP films, were calculated for both freshly prepared and degraded POAP films (column 4 in Table 1). On the basis of a degree of reduction defined as $\theta_{Red} = Q_{Red}(E)/Q_{T,Red}$, where $Q_{Red}(E)$ is the reduction charge at each *E* value assessed from *E* = 0.5 V towards the negative potential direction on the voltammetric responses (see Fig. 1) and $Q_{T,Red}$ = 2.8 mC cm^{-2}, a $\theta_{Red,Max}$value was calculated for freshly prepared and degraded POAP films (column 5 in Table 1). When the polymer film is only subjected to potential cycles within the range -0.2 V < *E* < 0.5 V (see curve (a) in Fig. 1) a maximum degree of reduction ($\theta_{Red,Max}$= 1, for $Q_{T,Red}$ = 2.8 mC cm^{-2}) is achieved, taking $Q_{T,Red}$ = 2.8 mC cm^{-2} as reference charge.

In these CV measurements a PAR model 173 potentiostat and a PAR Model 175 function generator were used. A X1-X2-Y Hewllet-Packard Model 7046 B Plotter was used to record the *j-E* responses.

1.3 RDEV Experiments with Both Fresh and Degraded Poap Films

With both freshly prepared and degraded POAP films obtained as indicated in sections *1.2.1* and *1.2.2*, respectively, RDEV experiments were performed in the presence of a solution containing equimolar concentrations of benzoquinone (Q) and hydroquinone (HQ) species. Firstly, stationary current-potential (*I-E*) curves at different electrode rotation rates Ω were recorded

Table 1: Maximum degrees of reduction $\theta_{Red,Max}$ obtained from POAP films deposited on a rotating gold disk electrode within the potential region of maximal electroactivity (-0.2 V < E < 0.5 V). Degraded POAP films are obtained after to subject freshly POAP films to potential cycling between -0.2 V and E_{upl} V.

Films	E^a_{upl}/V	Cycling time/min[b]	$Q^c_{T,Red}$ /mC cm^{-2}	$\theta^d_{Red,Max}$
Freshly prepared			2.8	1
Degraded films				
First group	1.0			
1		4	2.44	0.84
2		8	2.17	0.75
3		55	1.25	0.43
Second group	0.8			
4		6	2.58	0.89
5		12	2.38	0.82
6		35	2.06	0.71
7		70	1.60	0.55
Third group	0.65			
8		7	2.75	0.95
9		33	2.35	0.81
10		93	1.77	0.61
11		183	0.93	0.32

[a] Extreme positive potential value at which the POAP film was subjected to produce polymer degradation.

[b] Cycling time between the limits -0.2 V and E_{upl} V at which the corresponding POAP film was subjected (ν = 0.01 V s^{-1}).

[c] Maximal voltammetric reduction charge achieved by a POAP film within the potential region of maximal electroactivity of POAP after to be subjected to potential cycles within the range -0.2 V < E < E_{upl} V during the time period indicated in column 3. $Q_{T,Red}$ = 2.8 mC cm^{-2}, is the maximal reduction charge obtained for a freshly prepared POAP film only cycled within the potential range -0.2 V< *E* < 0.5 V.

[d] Maximum degree of reduction achieved by a POAP film within the potential region of maximal electroactivity of POAP after to be subjected to potential cycles between -0.2 V and E_{upl} V during the time period indicated in column 3. The value $\theta_{Red,Max}$ = 1 was considered as a reference value and it arises from the value $Q_{T,Red}$= 2.8 mC cm^{-2}, achieved for the POAP film only subjected to potential scans within the range -0.2 V < E < 0.5 V.

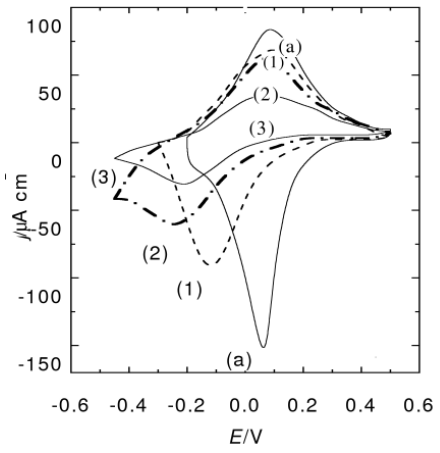

Figure 1: *j versus E* responses for a 2.8 mC cm^{-2} thick POAP film deposited on a 100 nm thick gold film. (a) A freshly prepared POAP film; (1)-(3) POAP films after being subjected to potential cycling within the range -0.2 V < *E* < 1.0 V for: (1) 4 min; (2) 8 min; (3) 55 min. Electrolyte: 0.1 M $HClO_4$ + 0.4 M $NaClO_4$. Scan rate: ν = 0.01 V s-1.

for a freshly prepared POAP film contacting a 0.1 M $HClO_4$ + 0.4 M $NaClO_4$ + 2 x 10^{-3}M (Q/HQ) solution. Secondly, the same experiment was consecutively repeated with the 11 degraded POAP films. Only cathodic *I-E* responses at potential values within the range -0.2 V < *E* < 0.0 V where Q reduction occurs at POAP films were considered here (see below). From these curves, the cathodic limiting current *vs.* electrode rotation speed ($I_{lim,c}$ *vs.* $\Omega^{1/2}$) dependencies were obtained for both freshly prepared and degraded POAP films.

These steady-state measurements were performed using the same measurement system indicated in section 1.2.2. The electrode rotation speed Ω was controlled with a home-made equipment that allows one to select a constant Ω in the range 50 rev min^{-1}< Ω < 10000 rev min^{-1}. This was periodically controlled with a digital phototachometer (Power Instruments Inc., model 891).

1.4 AC Impedance Experiments with Both Fresh and Degraded Poap Films

Impedance diagrams at potential values within the range -0.2 V < *E* < 0.0 V, corresponding to cathodic limiting currents where Q reduction proceeds on both freshly prepared and degraded POAP films, were recorded at selected Ω values. Also, *ac* impedance diagrams in the only presence of the supporting electrolyte (0.1 M $HClO_4$ + 0.4 M $NaClO_4$) were recorded within the same potential region. Impedance spectra were measured following 30 min application of the steady-state potential ranging from -0.2 V to 0.0 V. Impedance measurements in the frequency range 0.01 Hz and 10 kHz were performed with a PAR 309 System. The values of the impedances were determined at seven discrete frequencies per decade with a signal amplitude of 5 mV. The validation of the impedance spectra was done by using Kramers-Kronig transformations

1.5 Chemicals and Electrolyte Solutions

AR grade chemicals were used throughout. o-aminophenol (Fluka) was purified as described elsewhere [4,30]. $HClO_4$ and $NaClO_4$ Merck were used without further purification. Benzoquinone and hydroquinone Merck were also used without purification. The solutions were prepared with water purified using a Millipore Milli-Q system. The conductivity of the 0.1 M $HClO_4$ + 0.4 M $NaClO_4$ + 2 x 10^{-3} M (Q/HQ) solution was measured with a conventional *ac* bride Phillip PR 9500 at 1 kHz. A resistance value around $R_s \sim 1.09$ ohm cm^2 was obtained. This last resistance value was considered in the fitting of the experimental impedance diagrams by using the Vorotyntsev's model (see below).

2. RESULTS AND DISCUSSION

2.1 Different Behaviour of Freshly Prepared and Degraded Poap Films Under CV, RDEV and EIS Experiments

After degradation of POAP films (see for instance, *j-E* responses (1) to (3) in Fig.1) an attenuated reduction wave is observed as compared with the initial wave corresponding to the film only subjected to potential cycling within the range -0.2 V < *E* < 0.5 V (plot (a) in Fig. 1). This loss of electroactivity was considered as due to an oxidative polymer degradation [24,25]. The degradation of electroactive polymer films has been attributed to an excessive uptake of doping sites by dopant species from the electrolyte solution. These species may associate strongly with redox sites of the polymer chains resulting in electrostatic cross-linking. Thus, degradation results of the difficulty of recovering dopant species, which have diffused deeper into the polymer film. In this sense, degradation should lead to a mixed material, formed on the electrode surface, having an important electroactive fraction and also a degraded and non-electroactive part. It was proved that polymers, such as POAP and derivatives, are doped by hydrogen ions [9,15,26,31] rather than supporting electrolyte anions. Is is usually assumed that redox reactions of POAP modified electrodes result from protonation-deprotonation of polymer's nitrogen atoms [8,9,31,32] and also, the existence of mobile and immobile forms of hydrogen ions within the bulk of POAP films was considered to be probable [33]. The existence of some traps for hydrogen ions within the bulk of the polymer film which provide binding of the ions with polymer film fragments was also suggested [33]. Thus, it is possible that degradation of POAP were related to the fixation of hydrogen ions.

Concerning RDEV experiments, Fig. 2 (full circles) shows that for a freshly prepared POAP film contacting a HQ/Q solution,

a linear $I_{lim,c}$ *vs.* $\Omega^{1/2}$ dependence is obtained for the cathodic currents, within a wide range of Ω values. In previous work [34] RDEV experiments were performed to study the diffusion processes of benzoquinone (Q) and hydroquinone (HQ) species through freshly prepared POAP films. Diffusion limited-currents at $E < 0.0$ V for the Q reduction and at $E > 0.8$ V for the HQ oxidation were observed. Cathodic limiting currents for Q reduction (see inset in Fig. 2) were related to a rapid electron-transfer mediation at the POAP-redox active solution interface (without significant penetration of Q into the polymer layer). For freshly prepared POAP films, the cathodic limiting current is polymer film thickness independent and follows the Levich equation. Interpretation of these results was made on the basis of the membrane diffusion theory [34] and the electron-hopping model [35,36]. However, for degraded POAP films, as more degraded the polymer film the more attenuated is the limiting current at $E < 0.0$ V (see inset in Fig. 2). Also, for degraded POAP films, after a certain Ω value, a constant limiting current value $I_{lim,c}$ independent of Ω, is achieved (see, for instance, plots (1) to (3) in Fig. 2 for the three samples of the first group). This limiting current value at which $I_{lim,c}$ (= I_e) becomes constant was considered as a representation of the maximum flux of redox species (or electrons) confined in the polymer, according to Eq. (1) [37]:

$$I_e = nFAD_e(c/\phi_p) \quad (1)$$

This equation implies a constant gradient of redox species across the film (c/ϕ_p), where c is the concentration of redox sites of the polymer and ϕ_p the polymer film thickness. D_e represents a measure of the electron hopping rate and n express the numbers (fractions) of unit charges per monomer unit of the polymer. A is the electrode area and F the Faraday's constant. Then, such a constant value of the current (I_e) (Fig. 2) for degraded POAP films could be attributed to the slow electron transport across the POAP film to mediate in the electron-transfer reaction at the polymer-solution interface. This was explained in terms of a gradual increase in the hopping distance between redox sites with increasing the polymer degradation, which causes a D_e decrease [25] (see also Eq. (1)). In this sense, experimental results in [25] were interpreted assuming that a progressive degradation of POAP leads to an extensive production of inactive gaps giving rise to distributions of residual active redox sites, which are more expanded as more inactive becomes the polymer.

With regard to impedance experiments, at potential values within the range -0.2 V < E < 0.0 V, *ac* impedance diagrams at different Ω values for a degraded film of the first group and a freshly prepared film, are shown in Fig. 3 and Fig. 4 and its inset, respectively. While experimental impedance plots of freshly prepared POAP films exhibit only one semicircle, degraded films show two semicircles. Also, while for degraded POAP films the loop at low-frequency seems to be Ω dependent, the high-

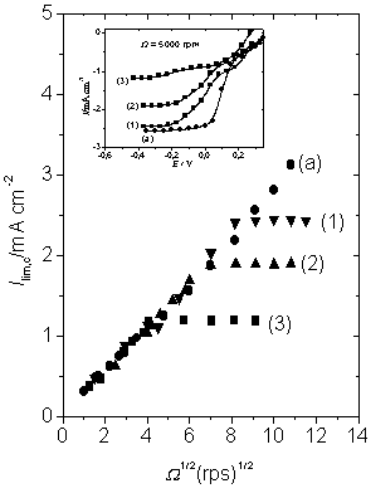

Figure 2: Levich representation $I_{lim,c}$ *versus* $\Omega^{\frac{1}{2}}$ for the cathodic plateau ($E < 0.0$ V) when POAP films contact a 0.1 M $HClO_4$ + 0.4 M $NaClO_4$.+ 2 x 10^{-3} M (HQ/Q) solution: (a) a freshly prepared POAP film and (1)-(3) the three degraded POAP films of the first group (Table 1). Thickness of POAP films: 60 nm. Inset: steady-state *I-E* curves at 5000 rpm for: (a) a fresh POAP film and (1)-(3) the three films of the first group. The same electrolyte indicated above.

frequency semicircle is independent of this variable. The size of the HF semicircle depends on the degree of polymer degradation ($\theta_{Red,Max}$). In this connection, at a given Ω value as higher the polymer degradation (lower $\theta_{Red,Max}$) the greater is the HF semicircle. In both cases, fresh and degraded POAP films, at high-frequency impedance diagrams in the presence of Q species tend to coincide with those obtained in the only presence of the supporting electrolyte [24].

2.2 Thick Poap Films Deposited on a Specular Gold Surface. Experimental Conditions to Apply an Homogenenous Impedance Model. The Impedance Model of Vorotyntsev et al. [27]

It is evident that the treatment of the impedance data is often complicated by accompanying not only experimental but also theoretical difficulties. With regard to experimental condition, by depositing a gold film on the gold disc as described in the experimental section, it is expected to reduce at an atomic scale surface defects of the gold disc base electrode, in such a way that the polymer film is deposited on an enough smooth surface. Gold films deposited under high vacuum conditions ($\sim 10^{-7}$ Torr), as in the present work, result polycrystalline with crystallite sizes between 0.01 and 0.1 μm [38-40]. Studying the "Size effects" [39] on these gold films, a value of the specularity parameter, $p \sim 0.91$, was estimated. p correlates with the roughness of the surface topography and the presence of surface

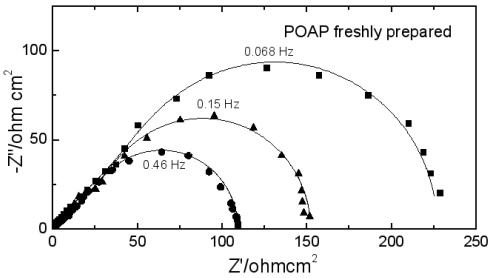

Figure 3: *Ac* impedance diagrams in the Nyquist co-ordinates (*-Z"vs. Z*) obtained at *E* = -0.2 V for a freshly prepared POAP film contacting a 0.1 M $HClO_4$ + 0.4 M $NaClO_4$ + 2 x 10^{-3} M (HQ/Q) solution. The different diagrams correspond to different electrode rotation rates, Ω: (■) 1180 rpm; (▲) 2600 rpm; (•) 5000 rpm. Discrete points are experimental data and continuous lines represent the fitting by using Eq. (2) [27].

defects. More precisely, this parameter represents the probability of an electron being reflected specularly or diffusely (due to the presence of defects) at the film surface. The *p* value ranges from 0 for complete diffuse scattering to 1 for complete specular scattering. Thus, imperfections should lead to experimental *p* values much lower than 1. In this connection *p* values of our gold films, deposited on the gold disc, are enough high ($p \sim$ 0.91) to assume a low amount of surface defects on an atomic scale, as compared with the surface of a bulk electrode mechanically polished (gold disc), to deposit a polymer film.

Concerning the structure of the polymer layer deposited on the metal electrode, it has been indicated that while open structures of electroactive polymer films allow incorporation of electrolyte into the polymer matrix, compact structures prevent its incorporation. In this connection, high permeability values of some polymer films [41] to transport of species from the solution in contact with the polymer to the metal substrate have been attributed to dispersed polymer structures with imperfections (*e.g.* pinholes and large channels) with dimensions large compared to those of species present in solution. On the basis of previous resistometric measurements [11,12], it was proved that when a 2.8 mC cm^{-2} thick POAP film covers a gold film, anions of the electrolyte do not interact directly with the base gold film electrode, which should be indicative of the existence of a relatively compact polymer layer on the gold film electrode. Also, in [15] it was demonstrated that porosity (or roughness) status of the polymer-solution layer for POAP films is stabilised with increasing the polymer thickness (thickness > 50 nm for POAP) and then, porosity effects are not to high for sufficiently high thick films. Then, the experimental arrangement used in this work, that is, a gold base electrode of low surface roughness ($p \sim$ 0.91 after deposition of a thin gold film by evaporation) coated with a 2.8 mC cm^{-2} thick POAP film, could be a good approximation to the existence of an homogeneous (uniform) polymer layer on an electrode surface to apply an homogeneous electrochemical model in its study. Then, the general theory of *ac* impedance described by Vorotyntsev et al. in [27] was employed to interpret experimental impedance data of this modified electrode system. This theory was developed within the framework of the assumption that the redox active species is only present in the solution phase but not inside the film, and they participate in the interfacial electron exchange with the polymer at the film-solution boundary. As in the present case, one has a modified electrode geometry with a redox active electrolyte solution (m|film|es), eq. (41) of Ref. [27] (Eq. (2) in this work) must be applied:

$$Z_{m|film|es} = R_{m|f} + R_f + R_s + [Z_e^{f|s} R_i^{f|s} + W_f Z_{12}^m] \\ (Z_e^{f|s} + R_i^{f|s} + 2W_f coth 2\nu)^{-1} \quad (2)$$

where

$$Z_{12}^m = Z_e^{f|s}[coth\nu + (t_e - t_i)^2 tanh\nu] \\ + R_i^{f|s} 4t_i^2 tanh\nu + W_f 4t_i^2 \quad (3)$$

In Eqs (2) and (3):

$\nu = [(j\omega\phi_p^2)/4D]^{1/2}$, is a dimensionless function of the frequency ω, ϕ_p is the film thickness, *D* is the binary electron-ion diffusion coefficient and $t_i$and t_e are the migration (high frequency) bulk-film transference numbers for anions and electrons, respectively. *D* is defined as $D = 2D_iD_e(D_e+D_i)^{-1}$ and $t_{i,e} = D_{i,e}(D_e+D_i)^{-1}$ where D_e and D_i are the diffusion coefficients for the electrons and ion species, respectively.

$W_f = [\nu/j\omega\phi_p C_p] = \Delta R_f/\nu$, is a Warburg impedance for the electron-anion transport inside the polymer film. ΔR_f ($= \phi_p/4DC_p$) is the amplitude of the Warburg impedance inside the film and C_p is the redox capacitance per unit volume.

$R_f(=\phi_p/\kappa)$ is the high-frequency bulk-film resistance, R_s the ohmic resistance of the bulk solution (κ is the high frequency bulk conductivity of the film), $R_{m|f}$ is the metal-film interfacial electron-transfer resistance and $R_i^{f|s}$ is the film-solution interfacial ion-transfer resistance.

$Z_e^{f|s} = (R_e^{f|s}+W_s)$, is the electronic impedance, where $R_e^{f|s}$ is the interfacial electron-transfer resistance at the film-solution interface and W_s is the convective diffusion impedance of redox species in solution, which contains the bulk concentrations of ox(red) forms, $c_{ox}(c_{red})$, and their diffusion coefficients inside the solution, $D_{ox}(D_{red})$. Also, it contains the Nernst layer thickness, δ.

$R_e^{f|s}$ is defined as:

$$R_e^{f|s} = RT\,(nF^2 k_o c_{red})^{-1} \quad (4)$$

where k_o is the rate constant of the reaction between the film and the redox active forms in solution. Diffusion of the redox forms from the bulk solution to the film-solution interface can be regarded as stationary through the diffusion layer thickness, expressed in cm by

$$\delta = 4.98 D_{ox,red}^{1/3} \eta^{1/6} \Omega^{-1/2} \quad (5)$$

where η is the kinematic viscosity of the solution in the same units as $D_{ox,red}$ and Ω the rotation rate of the disk electrode in rpm. The rest of the constants have their usual meaning.

This model also includes the impedance behaviour of the polymer contacting the inactive electrolyte (absence of the redox couple in solution) by considering $Z_e^{f|s} \rightarrow \infty$ in Eq. (2).

It should be indicated that this theory is strictly valid when charging of interfacial double layers is negligible. If it is not the case, a more complete model, such as developed by Vorotyntsev in [42], should have to be used. In [42], besides the traditional "double-layer" capacitance and interfacial charge transfer resistances, two additional parameters for each boundary, "interfacial numbers" for each species and "asymmetry factors", are introduced. However, it is well-known the mathematical difficulty of determining numerous parameters of a model from experimental data. Despite of this last theoretical limitation, we ensure, at least with a good approximation, the conditions assumed by the model described in [27] concerning a uniform and non porous film and no penetration of redox species from the solution. However, also, considering the mentioned limitation, to correctly describe the system, it should be expected some discrepancy between experimental and theoretical results.

2.2.1 Application of the impedance model of Vorotyntsev et al. [27]. Determination of the different charge transfer and charge transport parameters of POAP as functions of the degree of degradation, $\theta_{Red,Max}$.

Although in the present *ac* impedance study several experimental impedance diagrams in Nyquist co-ordinates (imaginary *versus* real part of the impedance) were recorded for each degraded and freshly prepared POAP film, for the sake of simplicity only complex impedance plane plots showed in Figs 3 and 4, are presented. These diagrams correspond to a freshly prepared film and the degraded film (1) (see Table 1), respectively, at different Ω values. In these diagrams besides the measured values (discrete points), the simulated curves (continuous lines) calculated by using Eq. (2) [27] are also displayed. As often is considered that some transformed curves could give more valuable information than Nyquist plots about the goodness of the fitting, real and imaginary parts *vs*. frequency plots correspondig to each Nyquist plot were are also built (not shown). In every impedance diagram was observed that while the fitting seems to be very good at low and high frequencies, it is clearly less satisfactory in the intermediate frequency region.

The fitting procedure by using Eq. (2) was based on the CNLS (Complex Non-Linear Squares) method. A rigorous fitting procedure was performed. Eight replicate measurements for each degraded POAP film were carried out and the error structure was assessed following the method recommended by Agarwal et al. [43-45] and Orazem [46]. In the present work the standard deviation for the real (σ_{Zr}) and imaginary (σ_{Zj}) parts of the impedance followed the form proposed by Orazem [46] (see eq. (8) of Ref. [46]):

$$\sigma_{Zr} = \sigma_{Zj} = \alpha|Zj| + \beta|Zr| + \gamma|Z|^2 Rm^{-1} + \delta \quad (6)$$

where *R*m is the current measuring resistor used for the experiment, *Z*r is the real part of the impedance and *Z*j is the imaginary part of the impedance. α, β, γ and δ are constant which have to be determined. The values of these scaling factors resulted: α = 5.77 x 10^{-3}, β = 0, γ = 3.7 x 10^{-5} and δ = 6.3 x 10^{-4}. The error structure was found to follow the same model within the degradation range $0.3 < \theta_{Red,Max} < 1$. At $\theta_{Red,Max}$ values lower than 0.3 the error structure model parameters had different values, but these results are not reported here. Then, continuous lines in Figs 3 and 4 represent the weighted complex non-linear least-squares fit to the data. The regression was weighted by the inverse of the variance of the stochastic part of the measurement. In all conditions the weighted sum of the square of the residuals was below one [46].

In the simulations the number of transferred electrons, *n*, was assumed to be 1 and diffusion coefficient values of the redox species (Q and HQ) were considered equals, $D_{ox,red}$ = 1.5 x 10^{-5} cm^2 s^{-1}. Also, the bulk concentrations of the redox substrate species were considered equals (c_{ox} = c_{red} = 2 x 10^{-6} mol cm^{-3}). On the basis on the reduction charge *vs*. ellipsometric thickness working curve reported in [1], the polymer thickness was considered as $\phi_p \sim 60$ nm. The value of the total redox site concentration of POAP was considered as c_o = 4.7 x 10^{-3} mol cm^{-3} [4]. As was indicated in the experimental section, the ohmic resistance of the solution in contact with the polymer films, R_S, was measured. A value $R_S \sim 1.09$ ohm cm^2 was obtained. Then, considering the high-frequency intercept of impedance diagrams of POAP films in the presence and absence of the redox couple in solution, as R_o, the high-frequency bulk POAP film resistance R_f was calculated as $R_f = R_o - R_S$ [47]. This last value varied within the range $1.02 < R_f < 2.6$ ohm cm^2 and it seems not to be strongly dependent

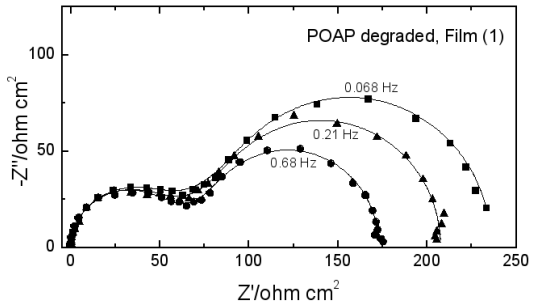

Figure 4: *Ac* impedance diagrams in the Nyquist co-ordinates (-*Z"vs*. *Z*) obtained at *E* = -0.2 V for the film (1) of the first group (see Table 1). Degree of degradation: $\theta_{Red,Max}$ = 0.84. The different diagrams correspond to different electrode rotation rates, Ω: (■) 2000 rpm; (▲) 3000 rpm: (●) 5000 rpm. Electrolyte: 0.1 M $HClO_4$ + 0.4 M $NaClO_4$+ 2 x 10^{-3} M (HQ/Q) solution. Discrete points are experimental data and continuous lines represent the fitting by using Eq. (2) [27].

on the degree of polymer degradation. Then, R_f and R_S values were imposed in the fitting. The remnant parameters contained in Eq. (2): $R_{m|f}$, $R_i^{f|s}$, $R_e^{f|s}$, C_p, D_e and D_i were calculated from the experimental impedance data by the fitting procedure above described. With regard to the three first parameters ($R_{m|f}$, $R_i^{f|s}$ and $R_e^{f|s}$) they were varied without restrains during the fitting. However, some reference values were considered for C_p, D_e and D_i. For POAP film thickness freshly prepared used in this work ($Q_{T,Red}$ = 2.8 mC cm^{-2}, ϕ_p = 60 nm) and solution pH = 1, D_e and D_i values were allowed to vary within the range 10^{-7}-10^{-11} cm^2 s^{-1}, in such a way that diffusion coefficient values lower than 10^{-11} were considered not realistic for these thick films. That is, D_e and D_i values lower than 10^{-11} were only obtained from impedance diagrams (not shown) of very thin POAP films ($Q_{T,Red}$ = 0.2 mC cm^{-2}, ϕ_p = 10 nm) contacting solutions of pH = 1, where it is possible an incomplete coating of the metal area by the thin polymer film. Concerning C_p, reference values were extracted from experimental -Z" *vs*. ω^{-1} slopes of impedance diagrams at sufficiently low frequency (in the absence of the redox substrate in solution) (see below). A contribution of the interfacial capacitance, C_H, also considered as a fitting parameter, was included in order to represent the actual impedance diagrams from the calculated ones.

The dependencies of the different charge transport and charge transfer parameters on $\theta_{Red,Max}$, extracted from the fitting procedure above described are shown in Figs 5 to 10. $R_{m|f}$ exhibits a strong increase from the beginning of the degradation, that is, from $\theta_{Red,Max}$ = 1 to $\theta_{Red,Max}$ = 0.5 (Fig. 5). At the same $\theta_{Red,Max}$ values, the ion-transfer resistance $R_i^{f|s}$ at the polymer-solution interface (Fig. 6) results almost one order of magnitude lower than $R_{m|f}$. Also, $R_i^{f|s}$ as a function of $\theta_{Red,Max}$ exhibits a different feature as compared with $R_{m|f}$. That is, while within the range 0.6 < $\theta_{Red,Max}$ < 1.0, $R_i^{f|s}$ remains nearly constant ($R_i^{f|s} \sim$ 10 ohm cm^2), a marked increase in $R_i^{f|s}$ is observed at the lowest $\theta_{Red,Max}$ values ($R_i^{f|s} \sim$ 40 ohm cm^2 for $\theta_{Red,Max} \sim$ 0.3). In the same way as $R_{m|f}$, a pronounced increase in the resistance related to the electron interfacial exchange $R_e^{f|s}$ at the polymer-solution interface, is observed from the beginning of the polymer degradation (high $\theta_{Red,Max}$ values) (Fig. 7). $R_e^{f|s}$ values were extracted from Eq. (4) using k_o as fitting parameter. The accuracy of $R_e^{f|s}$ values is somewhat affected, especially at the beginning of the degradation (high $\theta_{Red,Max}$ values) where the experimental situation $R_e^{f|s} \ll R_{m|f}$ (and even < $R_i^{f|s}$) predominates. Thus, $R_e^{f|s}$ values could be more realistic at high degrees of degradation (low $\theta_{Red,Max}$ values). Then, concerning the polymer-solution interface, a slow ion transfer process is observed for POAP as compared with the electron transfer process at this interface (compare Figs 6 and 7). Thus, even when the $R_{m|f}$ increase, during POAP degradation, affects strongly the diameter of the HF loop of the impedance diagrams (as reported previously [26]), this increase can also be associated to a $R_i^{f|s}$ increase [27]. With regard to C_H values, starting at a value around 17 μF cm^{-2}for a freshly prepared film, C_H decreased with increasing the degree of degradation of the polymer, reaching a value about 5 μF cm^{-2} for a almost completely degraded POAP film (Fig. 8). It is interesting to notice that in the same way as for $R_{m|f}$ and $R_e^{f|s}$, a more attenuated change on the C_H *vs*. $\theta_{Red,Max}$ dependence is observed at the lower $\theta_{Red,Max}$ values.

Similar differential behaviours observed between $R_i^{f|s}$ and $R_e^{f|s}$ with degradation (see Figs 6 and 7, respectively) are observed for the massive electron and ion transport. D_e and D_i changes with $\theta_{Red,Max}$ are shown in Figs 9 and 10, respectively. As can be seen, while D_e is strongly affected even at low degree of degradation (0.8 < $\theta_{Red,Max}$ < 1.0), D_i changes are more pronounced for $\theta_{Red,Max}$ < 0.6. It seems that a low degree of degradation should be enough to increase the hopping distance [25,48] and restrict strongly the electron motion within the polymer matrix. Taking into account that transfer and transport parameters obtained in this work correspond to the reduced state of POAP (-0.2 V < *E* < 0.0 V), it is possible that $R_i^{f|s}$ and D_i only reflect the proton movement through the polymer-electrolyte interface and inside the polymer film, respectively [14,15]. In this connection, the break at $\theta_{Red,Max} \sim$ 0.6, in the D_i*vs*. $\theta_{Red,Max}$ dependence could be related to the existence of two different forms (mobile and bound) of hydrogen ions in the bulk film, as was proposed in [15]. That is, after profound degradation, the mobile form of hydrogen ions, which is related to the film conductance, should be affected.

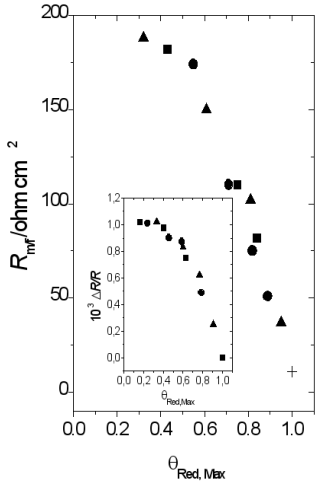

Figure 5: Metal-polymer interfacial electron-transfer resistance ($R_{m/f}$) as a function of the degree of degradation, $\theta_{Red,Max}$ for the 11 degraded POAP films indicated in Table 1: (■) films of the first group; (▲) films of the second group; (●) films of the third group. (+) Value corresponding to the freshly prepared POAP film. Electrolyte: 0.1 M $HClO_4$ + 0.4 M $NaClO_4$ + 2 x 10^{-3} M (HQ/Q) solution. Inset: Surface resistance change $\Delta R/R$ as a function of the degree of degradation, $\theta_{Red,Max}$ for the 11 degraded POAP films indicated in table 1 of [25]: (■) films of the first group; (▲) films of the second group; (●) films of the third group. Electrolyte: 0.1 M $HClO_4$ + 0.4 M $NaClO_4$+ 2 x 10^{-3} M (HQ/Q) solution. Scan rate: ν = 0.01 V s^{-1}.

From a quantitative point of view the Vorotyntsev's model gives D_e values near two orders of magnitude higher than D_i for POAP. Different reasons could be invoked to explain a fast electron motion relative to ion motion at POAP films. In the same way as was observed for Os(II) polyvinyl-bypyridile [49] and PANI films [50], it is possible that in POAP films also occurs a volume reduction during the redox switching, namely when going from the fully oxidised form to the reduced one. Thus, it is possible that electron hopping controls the charge transport process at POAP films in its oxidised state, where the polymer is swollen, which facilitates the ion transport [9]. However, in the present work, relative diffusion coefficient values ($D_e > D_i$) refer to the reduced state of POAP. That is, it is possible that our diffusion coefficient values correspond to POAP films that suffered a volume reduction due to their deswelling at the negative potential values corresponding to the reduced state. Then, under these conditions it is possible to explain a fast electron transport as compared with the proton transport in the present experiment, where POAP films are not enough swollen to facilitate the ion motion.

C_p *vs.* $\theta_{Red,Max}$dependence obtained by using Eq. (2) for the different degraded POAP films is shown in the inset of Fig. 8.

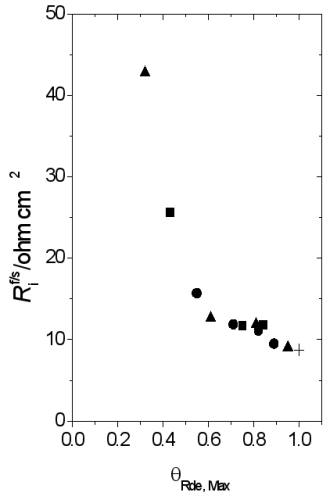

Figure 6: Polymer-solution interfacial ion-transfer resistance ($R_i^{f/s}$) as a function of the degree of degradation, $\theta_{Red,Max}$ for the 11 degraded POAP films indicated in Table 1: (■) films of the first group; (▲) films of the second group; (●) films of the third group. (+) Value corresponding to the freshly prepared POAP film. Electrolyte: 0.1 M $HClO_4$ + 0.4 M $NaClO_4$+ 2 x 10^{-3} M (HQ/Q) solution.

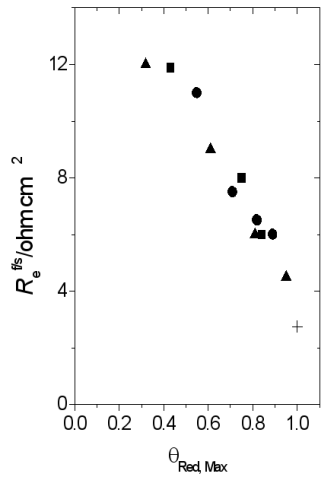

Figure 7: Interfacial electron-transfer resistance ($R_e^{f/s}$) at the polymer-solution interface as a function of the degree of degradation, $\theta_{Red,Max}$ for the 11 degraded POAP films indicated in Table 1: (■) films of the first group; (▲) films of the second group; (●) films of the third group. (+) Value corresponding to the freshly prepared POAP film. Electrolyte: 0.1 M $HClO_4$ + 0.4 M $NaClO_4$+ 2 x 10^{-3} M (HQ/Q) solution.

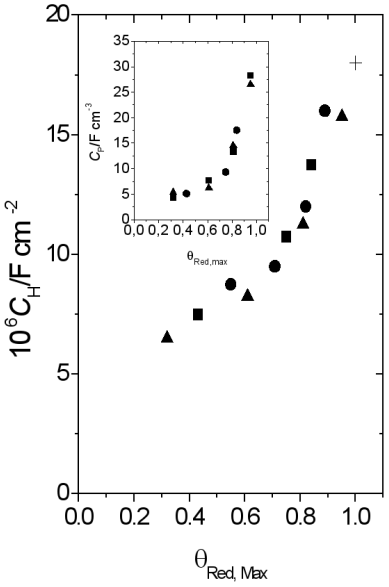

Figure 8: Interfacial capacitance (C_H) at the metal-polymer interface as a function of the degree of degradation, $\theta_{Red,Max}$ for the 11 degraded POAP films indicated in Table 1: (■) films of the first group; (▲) films of the second group; (●) films of the third group. (+) Value corresponding to the freshly prepared POAP film. Electrolyte: 0.1 M $HClO_4$ + 0.4 M $NaClO_4$+ 2 x 10^{-3} M (HQ/Q) solution. Inset: Redox capacitance (C_p) as a function of the degree of degradation, $\theta_{Red,Max}$ for the 11 degraded POAP films indicated in Table 1: (■) films of the first group; (▲) films of the second group; (●) films of the third group. (+) Value corresponding to the freshly prepared POAP film. Electrolyte: 0.1 M $HClO_4$ + 0.4 M $NaClO_4$+ 2 x 10^{-3} M (HQ/Q) solution.

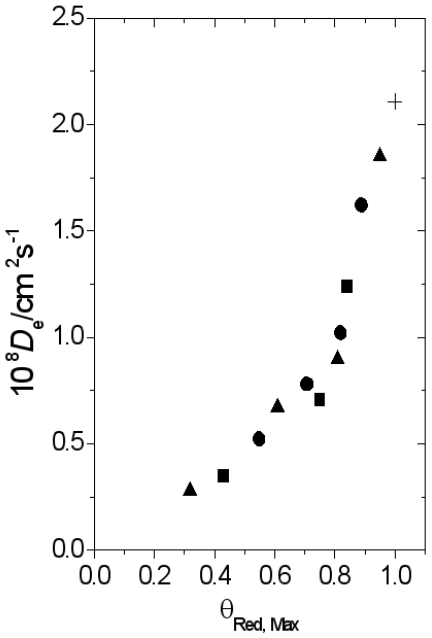

Figure 9: The electron diffusion coefficient (D_e) as a function of the degree of degradation, $\theta_{Red,Max}$ for the 11 degraded POAP films indicated in Table 1: (■) films of the first group; (▲) films of the second group; (●) films of the third group. (+) Value corresponding to the freshly POAP film. Electrolyte: 0.1 M $HClO_4$ + 0.4 M $NaClO_4$+ 2 x 10^{-3} M (HQ/Q) solution.

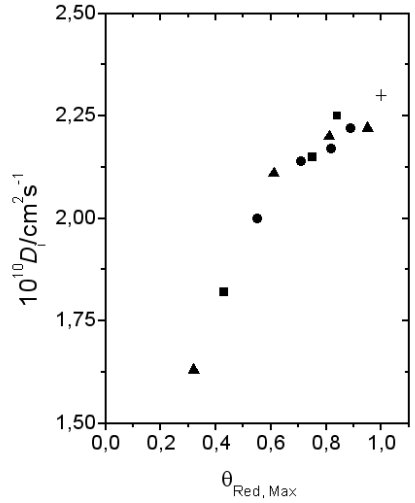

Figure 10: The ion diffusion coefficient (D_i) as a function of the degree of degradation, $\theta_{Red,Max}$ for the 11 degraded POAP films indicated in Table 1: (■) films of the first group; (▲) films of the second group; (●) films of the third group. (+) Value corresponding to the freshly POAP film. Electrolyte: 0.1 M $HClO_4$ + 0.4 M $NaClO_4$+ 2 x 10^{-3} M (HQ/Q) solution.

It can be seen that starting at a C_p value about 30 F cm^{-3}, for a freshly prepared film, a strong decrease of C_p up to $\theta_{Red,Max} \sim 0.8$ is observed. However, for higher degrees of degradation (lower $\theta_{Red,Max}$values) a more attenuated change is observed. Always, it should be kept in mind that these values correspond to the reduced state of POAP. There was no difference in the redox capacitance *vs.* $\theta_{Red,Max}$dependence achieved in the supporting electrolyte from the -Z" *vs.* ω^{-1} slopes and in the presence of the redox active substrate from Eq. (2). Only little differences in the numerical values of C_p were found. The good agreement between the redox capacitance values attained under these different conditions could be considered as an indication of the high fitting accuracy reached to obtain optimum parameters values (in this case C_p), for the treated system, by using Eq. (2). Also, the coherent behaviour between interfacial transfer processes and transport processes for a given entity (features of $R_e^{f|s}$ and D_e as functions of $\theta_{Red,Max}$for the electron (Figs 7 and 9) and features of $R_i^{f|s}$ and D_i as functions of $\theta_{Red,Max}$for the ion

(Figs 6 and 10) could be indicative of the suitability of the theoretical model of Vorotyntsev [27] to interpret the experimental impedance response of POAP, as compared with models used in previous works [7,24,26,51]. However, as was above emphasized, the fitting of experimental impedance spectra by means of the model described in [27], is not so good within the intermediate frequency region. This effect could be due to the fact that additional parameters of charging the double layers should be introduced to correctly describe a modified electrode system.

An interesting comparison can be stabilised between the $R_{m|f}$ *versus* $\theta_{Red,Max}$ dependence for different degraded POAP films obtained by impedance measurements in the present work (see Fig. 5) and the surface resistance change $\Delta R/R$ of thin gold film electrodes coated by different degraded POAP films (inset in Fig. 5) [12,25]. $\Delta R/R$ *versus* $\theta_{Red,Max}$ dependence was obtained from data reported in a previous work [25], where 11 POAP films were degraded by employing the same method as in the present work. As can be seen, similar features in $R_{m|f}$ *versus* $\theta_{Red,Max}$ and $\Delta R/R$ *versus* $\theta_{Red,Max}$ dependencies are observed. However, while $R_{m|f}$ is a transversal resistance at the metal-polymer interface related to the electron transfer process during the redox reaction of the polymer, $\Delta R/R$ changes were adjudicated to the scattering of conduction electrons from the inside of the metal to the metal-polymer interface, caused by changes in the translational symmetry parallel to the interface due to the presence of different distributions of redox sites at this interface (a more expanded distribution of redox sites as more degraded becomes the polymer) [12,25]. In this sense, $\Delta R/R$ changes are not the direct result of the electron transfer between the species on the metal surface electrode and the electrode, but rather that they originate from the effect of foreign surface particles on the conduction electrons of the metal itself [40]. Thus, despite the different origins of these two electron resistances at the polymer-metal interface and the different type of measurements by which their were obtained (*ac* impedance measurements and potentiodynamic potential scans at low scan rates, $\nu = 5 \times 10^{-3}$ Vs^{-1}), similar behaviours are observed as a function of the polymer degradation. This observation is interesting because it seems that a given surface process on the electrode affects in a similar way both the electron transport along (parallel) the metal surface and the electron transfer across the electrode-polymer interface.

At this point it should be indicated that the oxidation level reached by POAP films, when the potential limit is extended up to high positive values, could cause lateral reactions that alter the molecular structure of the polymer and, hence its properties. These reactions could increase the residual saturation in polymeric chains and conduction can occur mainly by intermolecular electron transfer between adjacent short segments instead of intramolecular conduction through conjugated domains in large polymeric chains. Under these conditions, parameters obtained in this work strictly represent fitting parameters of the model rather than real physical properties of the polymer.

CONCLUSION

The Electrochemical Impedance Spectroscopy was employed to study the degradation of poly-(o-aminophenol) films. The experimental arrangement employed in this work (a substrate base electrode free of a large amount of surface defects to deposit the films and the use of thick polyner films), was considered as suitable to apply an homogeneous impedance model, such as that of Vorotyntsev et al. [27], to interpret experimental impedance spectra obtained when freshly and degraded poly-(o-aminophenol) films contact a redox active couple in solution. The dependencies of the different charge transport and charge transfer parameters of the polymer on its degradation, were only extracted for the reduced state of the polymer and they exhibit different features. While some parameters are strongly affected from the beginning of the degradation, others only exhibit a strong variation for high degrees of degradation. The Vorotyntsev's model, applied to poly-(o-aminophenol), leads to a fast electron transport as compared with the ion transport and both of them become slower after degradation. Different decreases of D_e and D_i on the degree of degradation, were explained in terms of the different transport mechanisms proposed for the electron motion and the proton motion inside poly-o-aminophenol films. A marked break at a degree of degradation about 0.6, on the D_i *vs.* degree of degradation dependence could be adjudicated to different forms (mobile and bound) of hydrogen ions as was porposed for this polymer. A similar behaviour, in terms of degradation, was observed between the transversal charge transfer resistance at the metal-poly-(o-aminophenol) interface and the surface (lateral) resistance along this interface, the last calculated from the electron scattering mechanism for the conduction electrons in metals. It is expected that the results of this work can help to exploit more successfully the restrictive stability conditions of poly-(o-aninophenol) in its practical applications.

ACKNOWLEDGMENTS

The author gratefully acknowledges the Consejo Nacional de Investigaciones Científicas y Técnicas (CONICET) and also the Facultad de Ciencias Exactas, National University of La Plata (UNLP).

REFERENCES

[1] C. Barbero, J. Zerbino, L. Sereno, D. Posadas, Electrochim. Acta, 32, 693 (1987).

[2] T. Ohsaka, S. Kunimura, N. Oyama, Electrochim. Acta, 33, 639 (1988).

[3] A. Guenbourg, A. Kacemi, A. Benbachir, L. Aries, Prog. Org. Coat., 38, 121 (2000).

[4] C. Barbero, J.J. Silber, L. Sereno, J. Electroanal. Chem., 263, 333 (1989).

[5] S. Kunimura, T. Ohsaka, N. Oyama, Macromolecules, 21, 894 (1988).

[6] Y. Yang, Z. Lin, Synth. Met., 78, 111 (1996).

[7] C. Barbero, R.I. Tucceri, D. Posadas, J.J. Silber, L. Sereno, Electrochim. Acta, 40, 1037 (1995).

[8] R.I. Tucceri, C. Barbero, J.J. Silber, L. Sereno, D. Posadas, Electrochim. Acta, 42, 919 (1997).

[9] T. Komura, Y. Ito, T. Yamaguti, K. Takahasi, Electrochim. Acta, 43, 723 (1998).

[10] J.M. Ortega, Thin Solid Films, 371,28 (2000).

[11] R.I. Tucceri, J. Electroanal. Chem., 505, 72 (2001).

[12] R.I. Tucceri, J. Electroanal. Chem., 543, 61 (2003).

[13] H.J. Salavagione, J. Arias, P. Garcés, E. Morallón, C. Barbero, J.L. Vázquez, J. Electroanal Chem., 565, 375 (2004).

[14] H.J. Salavagione, J. Arias-Padilla, J.M. Pérez, J.L. Vázquez, E. Morallón, M.C. Miras, C. Barbero, J. Electroanal Chem., 576, 139 (2005).

[15] O. Levin, V. Kondratiev, V. Malev, Electrochim. Acta, 50, 1573 (2005).

[16] N. Hernández, J.M. Ortega, M. Choy, R. Ortíz, J. Electroanal. Chem., 515, 123 (2001).

[17] A.Q. Zhang, C.Q. Cui, J.Y. Lee, J. Electroanal. Chem., 413, 143 (1996).

[18] J. Yano, H. Kawakami, S. Yamasaki, Y. Kanno, J. of the Electrochemical Society, 148, E61-E65 (2001).

[19] M.J. Lobo, A.J. Miranda, J.M. López-Fonseca, P. Tuñón, Analytica Chimica Acta, 325, 33 (1996).

[20] M.A. Valdés García, P. Tuñón Blanco, A. Ivaska, Electrochim. Acta, 43, 3533 (1998).

[21] D. Pan, J. Chen, L. Nie, W. Tao, S. Yao, Electrochim. Acta, 49, 795 (2004).

[22] M.S. Golabi, A. Nozad, Electroanalysis, 15, 278 (2003).

[23] M.C. Miras, A. Badano, M.M. Bruno, C. Barbero, Portugaliae Electrochimica Acta, 21, 235 (2003).

[24] J.F. Rodríguez Nieto, R.I. Tucceri, D. Posadas, J. Electroanal. Chem., 403, 241 (1996).

[25] R. Tucceri, J. Electroanal. Chem., 562, 173 (2004).

[26] F.J. Rodríguez Nieto, R. Tucceri, J. Electroanal. Chem., 416, 1 (1996).

[27] M.A. Vorotyntsev, C. Deslouis, M.M. Musiani, B. Tribollet, K. Aoki, Electrochim. Acta, 44, 2105 (1999).

[28] R.I. Tucceri, D. Posadas, J. Electroanal. Chem., 191, 387 (1985).

[29] K.L. Chopra, “Thin Film Phenomena”, McGraw-Hill Co., New York, 1969.

[30] C. Barbero, J.J. Silber, L. Sereno, J. Electroanal. Chem., 291, 81 (1990).

[31] T. Komura, Y. Funahasi, T. Yamaguti, K. Takahasi, J. Electroanal. Chem., 446, 113 (1998).

[32] L.-L. Wu, J. Luo, Z.-H. Lin, J. Electroanal. Chem., 471, 53 (1996).

[33] M.A. Vorotyntsev, E. Vieil, J. Heinze, J. Electroanal. Chem., 450, 121 (1998).

[34] A. Bonfranceschi, A. Pérez Córdoba, S. Keunchkarian, S. Zapata, R. Tucceri, J. Electroanal. Chem., 477, 1 (1999).

[35] C.P. Andrieux, J.M. Savéant, J. Electroanal. Chem., 111, 377 (1980).

[36] E. Laviron, J. Electroanal. Chem., 112, 1 (1980).

[37] C. Deslouis, B. Tribollet, in “Advances in Electrochemical Science and Engineering”, Eds, H. Gerischer, C. Tobias, vol. 2, VCH Publishers, New York, USA, 1992, p. 205.

[38] F.M. Romeo, R.I. Tucceri, D. Posadas, Surf. Sci., 203, 186 (1988).

[39] K. Fuchs, proc. Camb., Phil. Soc. Math. Phys. Sci., 34, 100 (1938).

[40] R. Tucceri, Surface Science Reports, 56, 85 (2004).

[41] T. Ikeda, R. Schmehl, P. Denisevich, K. Willman, R.W. Murray, J. Am. Chem. Soc., 104, 2683 (1982).

[42] M.A. Vorotyntsev, Electrochim. Acta, 47, 2071, (2002).

[43] P.Agarwal, M.E. Orazem, L.H. García-Rubio, J. Electrochem. Soc., 139, 1917 (1992).

[44] P.Agarwal, O.D. Crisalle, M.E. Orazem, L.H. García-Rubio, J. Electrochem. Soc., 142, 4149 (1995).

[45] P.Agarwal, M.E. Orazem, L.H. García-Rubio, J. Electrochem. Soc., 142, 4159 (1995).

[46] M.E. Orazem, J.Electroanal. Chem., 572, 317 (2004).

[47] M.M. Musiani, Electrochim. Acta, 35, 1665 (1990).

[48] Ch.E.D. Chidsey, R.W. Murray, J. Phys. Chem., 90, 1479 (1986).

[49] G. Ybarra, C.Moina, F.V. Molina, M.I. Florit, D. Posadas, Electrochim. Acta, 50, 1505 (2005).

[50] L. Lizarraga, E.M. Andrade, F.V. Molina, J. Electroanal. Chem., 561, 127 (2004).

[51] F.J. Rodríguez Nieto, D. Posadas, R. Tucceri, J. Electroanal. Chem., 434, 83 (1997).